Coarsening of metal oxide nanoparticles

Gerko Oskam,[1,*] Zeshan Hu,[1] R. Lee Penn,[2] Noshir Pesika,[3] and Peter C. Searson[1,†]
[1]*Department of Materials Science and Engineering, Johns Hopkins University, Baltimore, Maryland 21218*
[2]*Department of Earth and Planetary Sciences Science and Engineering, Johns Hopkins University, Baltimore, Maryland 21218*
[3]*Department of Chemical Engineering, Johns Hopkins University, Baltimore, Maryland 21218*
(Received 4 March 2002; published 24 July 2002)

In solution phase synthesis of nanoparticles, processes such as coarsening and aggregation can compete with nucleation and growth in modifying the particle size distribution in the system. We show that coarsening of ZnO and TiO_2 nanoparticles in solution follows the Lifshitz-Slyozov-Wagner rate law for diffusion controlled coarsening originally derived for colloidal systems with micrometer-sized particles, where the average particle size cubed is proportional to time. The rate constant for growth of ZnO in propanol is in the range 10^{-4}–10^{-2} $nm^3\,s^{-1}$ and is dependent on the precursor anion and temperature. The coarsening of TiO_2 nanoparticles from aqueous Ti(IV) alkoxide solutions is slower due to the low solubility of TiO_2 with the rate constant in the range 10^{-5}–10^{-3} $nm^3\,s^{-1}$ for temperatures between 150 °C and 220 °C. Epitaxial attachment of TiO_2 particles becomes significant at higher temperatures and longer times. We show that the dominant parameters controlling the coarsening kinetics are solvent, precursor salt, and temperature.

DOI: 10.1103/PhysRevE.66.011403 PACS number(s): 82.70.Dd, 81.10.Dn, 81.10.Aj

Solution phase methods have become widely used for the synthesis of metal and semiconductor nanoparticles [1–3], however, the parameters that control particle size remain poorly understood. Control of particle size is important since when the size of a particle is less than a characteristic length of interest (e.g., exciton diameter or electron mean free path) significant deviations from bulk behavior can be obtained. Thus, in order to tailor the optical, electrical, chemical, and magnetic properties of nanoparticles for specific applications, it is essential to develop a fundamental understanding of parameters that control particle size.

In this paper, we show that the coarsening of ZnO and TiO_2 nanoparticles from homogeneous solution follows the rate law derived by Lifshitz, Slyozov, and Wagner (LSW) [4,5] for micrometer-sized colloidal particles. The synthesis of ZnO is an example of a simple precipitation reaction where a soluble zinc salt reacts with hydroxyl ions or water [6,7], whereas the synthesis of TiO_2 is an example of hydrolysis of an alkoxide precursor followed by a condensation reaction [8–10].

In solution phase synthesis, processes such as coarsening and aggregation can compete with nucleation and growth in modifying the particle size distribution in the system. After injection of the reactants, nucleation is followed by particle growth until the supersaturation is depleted. If nucleation and growth are fast, coarsening and aggregation can dominate the time evolution of the particle size distribution. Aggregation is dependent on surface chemistry resulting in either oriented or random attachment of particles. Random aggregation usually leads to the formation of porous clusters of particles whereas epitaxial attachment of particles leads to the formation of secondary particles with complex shapes and unique morphologies [11–14].

Coarsening involves the growth of larger crystals at the expense of smaller crystals and is governed by capillary effects [4,5]. Since the chemical potential of a particle increases with decreasing particle size, the equilibrium solute concentration for a small particle is much higher than for a large particle, as described by the Gibbs-Thompson equation,

$$c_r = c_{r=\infty} \exp\left(\frac{2\gamma V_m}{RT}\frac{1}{r}\right), \tag{1}$$

where c_r is the equilibrium concentration for a spherical particle with radius r, $c_{r=\infty}$ is the equilibrium concentration at a flat surface (i.e., the bulk solubility), γ is the surface energy, and V_m is the molar volume. The resulting concentration gradients lead to the transport of solute (e.g., metal ions) from the small particles to the larger particles. The rate law for diffusion limited coarsening is obtained by inserting the linearized Gibbs-Thompson equation [assuming that $(2\gamma V_m/rRT)<1$] into Fick's first law [4,5],

$$\bar{r}^3 - \bar{r}_0^3 = kt, \tag{2}$$

where $\bar{r}$ is the average particle radius, $\bar{r}_0$ is the average initial particle size, t is time, and k is the rate constant.

Figure 1 shows absorption spectra for the synthesis of ZnO from $Zn(CH_3CO_2)_2$ and NaOH in 2-propanol at 35 °C as a function of time. The spectra show a well-defined exciton peak and a sharp absorption onset. The absorption onset at short times is significantly blueshifted from the bulk value (about 385 nm) illustrating that the particles are in the quantum regime. The absorption onset redshifts with time due to particle growth and coarsening. Note that the magnitude of the absorbance is constant, even at short times immediately after injection of the reactants, showing that nucleation is fast in comparison to growth.

*Present address: Departamento de Física Aplicada, CINVESTAV-IPN Unidad Mérida, A. P. 73 Cordemex, Mérida, Yucatán 97310, Mexico.
†Author to whom correspondence should be addressed; searson@jhu.edu

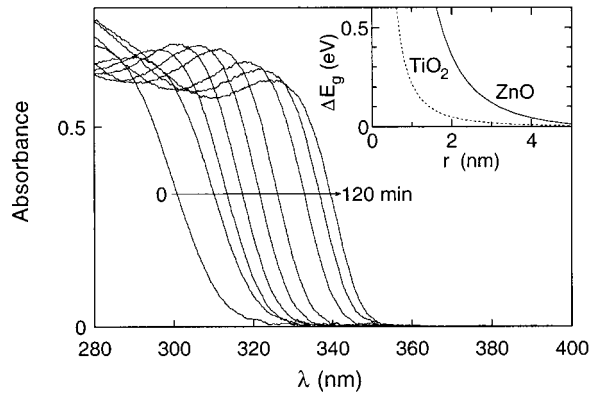

FIG. 1. Absorption spectra for the synthesis of ZnO nanoparticles from $Zn(CH_3CO_2)_2$ solution in 2-propanol at 35 °C. Sodium hydroxide and zinc salt solutions were adjusted to the growth temperature using a water bath and were then mixed under vigorous stirring to give 1m*M* Zn(II) and 1.6m*M* NaOH corresponding to 25% excess of Zn(II). Spectra are shown as a function of time after mixing of the solutions at 0, 2, 4, 8, 16, 30, 65, 90, and 120 min. The inset shows the shift in the band gap as a function of particle radius calculated from Eq. (3) using $m_e=0.26$, $m_h=0.59$, $E_g=3.2$ eV, and $\varepsilon=8.5$ for ZnO and $m_e=9$, $m_h=2$, $E_g=3.2$ eV, and $\varepsilon=170$ for TiO_2.

The average particle size in suspension can be obtained from the absorption onset using the effective mass model [15] where the band gap E^* (in eV) can be approximated by

$$E^*=E_g^{\text{bulk}}+\frac{h^2}{8er^2}\left(\frac{1}{m_e m_0}+\frac{1}{m_h m_0}\right)-\frac{1.8e}{4\pi\varepsilon\varepsilon_0 r}-\frac{0.124e^3}{h^2(2\varepsilon\varepsilon_0)^2}\left(\frac{1}{m_e m_0}+\frac{1}{m_h m_0}\right)^{-1}, \quad (3)$$

where E_g^{bulk} is the bulk band gap, h is Plank's constant, r is the particle radius, m_e is the electron effective mass, m_h is the hole effective mass, m_0 is free electron mass, e is the charge on the electron, ε is the relative permittivity, and ε_0 is the permittivity of free space. Due to the relatively small effective masses for ZnO ($m_e=0.26$, $m_h=0.59$ [16,17]) quantum effects are expected to occur for relatively large particle sizes. The inset of Fig. 1 shows the dependence of the band gap on particle radius according to Eq. (3) showing that ZnO particles exhibit significant confinement effects for particle radii less than about 4 nm. While there are a number of assumptions in using this method for determining particle size, the validity of this approach was confirmed from analysis of high-resolution transmission electron microscopy (TEM) images.

Figure 2 shows the time dependence of the average particle radius obtained from the absorption onset for the synthesis of ZnO from $Zn(CH_3CO_2)_2$ in propanol at different temperatures. The initial particle radius is about 1.5 nm, and the growth rate increases with increasing temperature. Figure 3 shows the growth data from Fig. 2 replotted as $\bar{r}^3$ vs time illustrating that the kinetics at longer times follow the LSW model for coarsening. Thus the increase in particle size in this regime occurs by the diffusion-limited transport of metal

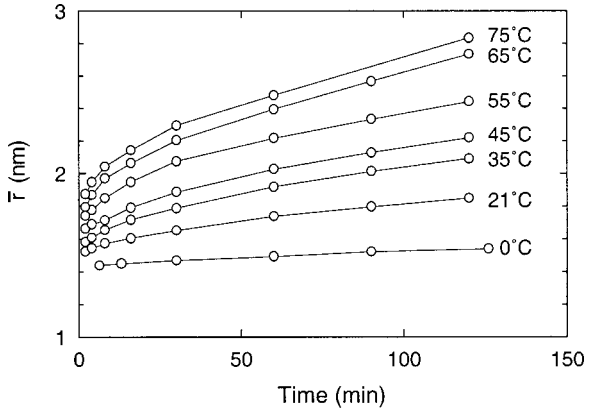

FIG. 2. Particle radius vs time for the synthesis of ZnO particles from $Zn(CH_3CO_2)_2$ solution in 2-propanol as a function of temperature.

ions from the higher concentration regions around small particles to the larger particles. The dependence of particle size on time shown in Fig. 3 suggests that growth resulting from the supersaturation is completed very quickly after nucleation such that coarsening is the dominant process at longer times.

The influence of the $Zn(CH_3CO_2)_2$ concentration was evaluated by repeating these experiments for initial concentrations of 0.5m*M*, 0.75m*M*, and 1.25m*M* while keeping the $Zn(CH_3CO_2)_2$/NaOH concentration ratio fixed. The $\bar{r}$ vs t curves were independent of the precursor concentration and, hence, particle concentration, indicating that interparticle effects are negligible in this concentration range.

Also shown in Fig. 3 are the curves for growth of ZnO from $Zn(ClO_4)_2$ and $ZnBr_2$ at the same temperature, illustrating that coarsening is fastest for synthesis from $Zn(ClO_4)_2$ and is slowest from $ZnBr_2$. This difference is related to anion adsorption; in general halide ions adsorb more strongly on surfaces than acetate ions, and perchlorate exhibits very weak surface interactions [18]. In the gas phase, acetic acid is known to displace ethanol and dissociatively adsorb on ZnO surfaces [19], and hence it is not surprising that acetate ions are adsorbed on the surface of the particles in propanol.

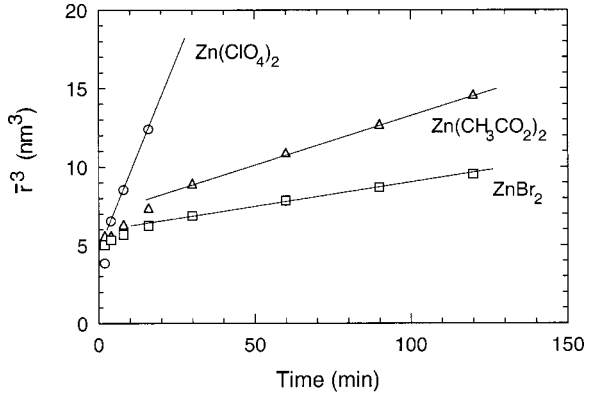

FIG. 3. The particle radius cubed vs time for the synthesis of ZnO particles at 55 °C from bromide, acetate, and perchlorate solution in 2-propanol.

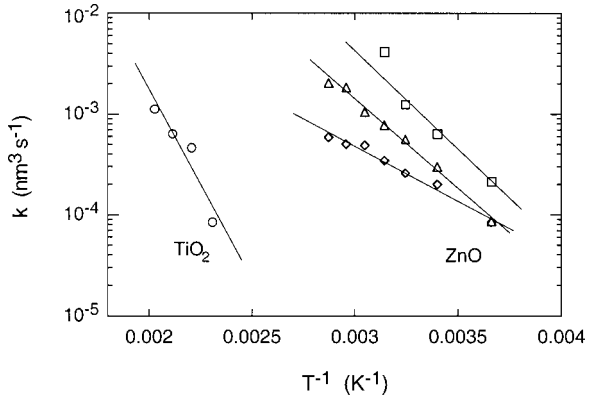

FIG. 4. The rate constant k vs reciprocal temperature for the coarsening of ZnO from ($\diamond$) bromide, ($\triangle$) acetate, and ($\square$) perchlorate solution, and for the growth of TiO_2 in aqueous nitrate solution.

Figure 4 shows the temperature dependence of the rate constants for coarsening on an Arrhenius plot. The rate constants k, obtained from the slopes of the linear regions of the plots of $\bar{r}^3$ vs time, are in the range of 10^{-4}–10^{-2} $nm^3\,s^{-1}$ and increase with increasing temperature. The activation energies obtained from the slopes are 0.21, 0.35, and 0.46 eV for bromide, acetate, and perchlorate solution, respectively.

Figure 5(a) shows $\bar{r}^3$ vs time for growth of TiO_2 at 160 °C and 200 °C, illustrating that this system is also dominated by coarsening, with the rate constant increasing with increasing temperature. The average particle radius immediately after nucleation was 1.55 nm. Further growth was achieved by heating the colloid at an elevated temperature in a closed titanium pressure vessel. The resulting colloid had a TiO_2 concentration of about 80 $g\,L^{-1}$, and x-ray diffraction showed that more than 90% of the particles were anatase, with the remainder brookite [20]. The average particle size was determined from transmission electron microscopy images. The particle size for TiO_2 cannot be obtained from absorbance measurements due to the relatively large effective masses ($m_e=9$ and $m_h=2$ [21,22]). This is illustrated in the inset of Fig. 1 that shows that quantum effects are expected at particles with radii smaller than about 2 nm.

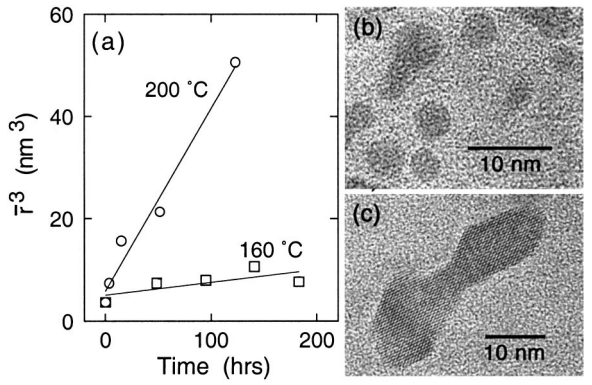

FIG. 5. (a) Particle radius cubed vs time for the coarsening of TiO_2 particles from aqueous nitrate solution at 160 °C and 200 °C. A typical procedure for the synthesis of TiO_2 nanoparticles was as follows: 15 mL of Ti-(O-*i*-Pr)$_4$ was added dropwise to 185 ml of distilled, deionized water acidified with 1.3 mL of concentrated HNO_3 with vigorous stirring at room temperature. The colloidal suspension was then peptized at 85 °C with stirring in an open flask for about 12 h. Also shown are two TEM images for TiO_2 particles grown at 160 °C for 15 h illustrating (b) single, primary particles, and (c) a secondary particle formed by epitaxial attachment of at least three primary particles. TEM samples were prepared by diluting the colloid by 100 000 with 1m*M* HNO_3 in water, and evaporative deposition on holey carbon coated copper grids. The average particle size was determined by measuring at least 500 particles from at least 10 TEM images.

Figure 5 also shows two high-resolution transmission electron microscope images of TiO_2 particles synthesized at 160 °C for 15 h. Most particles are primary particles as shown in Fig. 5(b), however, epitaxially attached particles are also observed [Fig. 5(c)]. Epitaxial attachment has been reported previously for solution phase synthesis of TiO_2, and in chloride solutions chains of particles of up to 100 nm in length consisting of more than 20 particles have been observed [11–13]. Since the attachment process in nitrate solution is relatively slow, the rate constant for coarsening of primary particles can be determined from the TEM images. Figure 4 also shows the rate constant for coarsening of TiO_2 in an Arrhenius plot, illustrating that k is strongly temperature dependent. The activation energy determined from the plot is found to be 0.75 eV, significantly higher than for growth of ZnO.

The difference in the coarsening kinetics between ZnO and TiO_2 can be determined by analysis of the rate constant. The rate constant k in Eq. (2) is given by

$$k=\frac{8\gamma V_m^2 c_{r=\infty}}{54\pi\eta a N_A}, \tag{4}$$

where η is the viscosity of the solvent, a is the solvated ion radius, and N_A is Avogadro's number. The viscosity is introduced into Eq. (4) by eliminating the diffusion coefficient using the Stokes-Einstein equation. The surface energy for the solid-vapor interface for metal oxides is on the order of 1 $J\,m^{-2}$ [23–26], however, electrostatic and chemical interactions at the solid-liquid interface are expected to reduce the surface energy to values in the range 0.1–0.5 $J\,m^{-2}$ [27]. Taking $\gamma=0.1\,J\,m^{-2}$ we obtain $2\gamma V_m/RT=1.2$ nm (for ZnO at 20 °C and for TiO_2 at 140 °C) illustrating that we are close to the limit of the LSW model's assumption that the Gibbs-Thompson equation can be linearized.

The temperature dependence of the rate constant can be evaluated in the following way. The molar volume, surface energy, and the solvated ion radius are weakly dependent on temperature, and hence the temperature dependence of the rate constant is expected to be dominated by the equilibrium concentration ($c_{r=\infty}$) and the solvent viscosity (η). The viscosity of 2-propanol is strongly temperature dependent [28], and accounts for a large part of the temperature dependence of the rate constant for ZnO. The dependence of the rate constant on the anion suggests that adsorption leads to a decrease in the equilibrium concentration and/or the surface energy resulting in a decrease in the magnitude of the rate constant. The temperature dependence of the viscosity of wa-

ter is relatively weak [29], implying that the temperature dependence of the rate constant for growth of TiO_2 is determined by the temperature dependence of the equilibrium concentration.

Substituting values for γ, V_m, a, and η, the bulk solubility $c_{r=\infty}$ can be obtained from the experimentally determined rate constants. For the growth of ZnO, the solubility is dependent on the salt used: taking $\gamma = 0.1\ \mathrm{J\,m^{-2}}$, $a = 0.51$ nm [30], $V_m = 14.8\ \mathrm{cm^3\,mol^{-1}}$, and the viscosity of 2-propanol, the solubility of ZnO is determined to be between 3×10^{-11} and $3 \times 10^{-10}\ \mathrm{mol\,L^{-1}}$, depending on the anion and temperature. These concentrations are below the detection limit of most experimental methods, however, the solubility of ZnO in water is relatively high so that measurements in 2-propanol/water mixtures can be used to provide an upper limit of the solubility in 2-propanol. From atomic absorption spectroscopy we have determined that the solubility of ZnO in water is $49 \times 10^{-6}\ \mathrm{mol\,L^{-1}}$ in good agreement with values reported in the literature [31]. With decreasing water concentration, the solubility decreases and is less than the detection limit ($10^{-6}\ \mathrm{mol\,L^{-1}}$) at concentrations less than 60 vol %. Thus the equilibrium solubility determined from the coarsening rate constant is less than the upper limit determined for 2-propanol/water mixtures with 60% water. We note that the growth of ZnO in water is fast and poorly controlled indicating that controlled growth is only achieved in nonaqueous or mixed solvents where the solubility is sufficiently low.

The equilibrium solubility of TiO_2, determined from the rate constants for coarsening between 160 °C and 220 °C, are in the range 4×10^{-13}–$4 \times 10^{-12}\ \mathrm{mol\,L^{-1}}$. The solubility of TiO_2 in phosphate buffer at pH 10 is on the order of $10^{-9}\ \mathrm{mol\,L^{-1}}$ at 200 °C and is dependent on phosphate ion concentration [32]. The solubility of TiO_2 in acidic solutions is known to be lower than in basic solutions suggesting that the values determined from the coarsening rate constants are reasonable.

In summary, the synthesis of ZnO and TiO_2 nanoparticles involves fast nucleation and growth followed by coarsening and/or aggregation. The dominant parameters controlling the coarsening kinetics are solvent, precursor salt, and temperature. All three of these parameters influence the equilibrium concentration of the metal ion complex. The precursor salt influences the equilibrium concentration of the metal ion complex through absorption of the anion. The choice of solvent and temperature influence the viscosity and hence the diffusion coefficient of the metal ion complex.

The authors gratefully acknowledge support from the JHU MRSEC (NSF Grant No. DMR00-80031).

[1] A. Henglein, Top. Curr. Chem. **143**, 113 (1988).
[2] A. P. Alivisatos, J. Phys. Chem. **100**, 13 226 (1996).
[3] C. B. Murray, C. R. Kagan, and M. G. Bawendi, Annu. Rev. Mater. Sci. **30**, 545 (2000).
[4] I. M. Lifshitz and V. V. Slyozov, J. Phys. Chem. Solids **19**, 35 (1961).
[5] C. Wagner, Z. Elektrochem. **65**, 581 (1961).
[6] D. W. Bahnemann, C. Kormann, and M. R. Hoffmann, J. Phys. Chem. **91**, 3789 (1987).
[7] E. M. Wong, J. E. Bonevich, and P. C. Searson, J. Phys. Chem. B **102**, 7770 (1998).
[8] C. Kormann, D. W. Bahnemann, and M. R. Hoffmann, J. Phys. Chem. **92**, 5196 (1988).
[9] D. Vorkapic and T. Matsoukas, J. Am. Ceram. Soc. **81**, 2815 (1998).
[10] A. Zaban, S. T. Aruna, S. Tirosh, B. A. Gregg, and Y. Mastai, J. Phys. Chem. B **104**, 4130 (2000).
[11] R. L. Penn and J. F. Banfield, Science **281**, 969 (1998).
[12] J. F. Banfield, S. A. Welch, H. Zhang, T. Thomsen Ebert, and R. L. Penn, Science **289**, 751 (2000).
[13] A. P. Alivisatos, Science **289**, 736 (2000).
[14] R. L. Penn, G. Oskam, J. Strathmann, P. C. Searson, A. T. Stone, and D. R. Veblen, J. Phys. Chem. B **105**, 2177 (2001).
[15] L. E. Brus, J. Phys. Chem. **90**, 2555 (1986).
[16] S. Shionoya, in *Phosphor Handbook*, edited by S. Shionoya and W. M. Yen (CRC Press, Boca Raton, FL 1998).
[17] L. I. Berger, *Semiconductor Materials* (CRC Press, Boca Raton, FL 1997), p. 184.
[18] A. W. Adamson, *Physical Chemistry of Surfaces*, 5th ed. (Wiley, New York, 1990).
[19] R. N. Spitz, J. E. Barton, M. A. Barteau, R. H. Staley, and A. W. Sleight, J. Phys. Chem. **90**, 4067 (1986).
[20] G. Oskam and P. C. Searson (unpublished).
[21] J. Pascual, J. Camassel, and H. Mathieu, Phys. Rev. B **18**, 5606 (1978).
[22] G. A. Acket and J. Volger, Physica (Amsterdam) **32**, 1680 (1966).
[23] A. A. Gribb and J. F. Banfield, Am. Mineral. **82**, 717 (1997).
[24] X. G. Wang, W. Weiss, Sh. K. Shaikhutdinov, M. Riter, M. Petersen, F. Wagner, R. Schlogl, and M. Scheffler, Phys. Rev. Lett. **81**, 1038 (1998).
[25] I. Manassidis, A. De Vita, and M. J. Gillan, Surf. Sci. Lett. **285**, L517 (1993).
[26] D. A. Weirauch and P. D. Ownby, J. Adhes. Sci. Technol. **13**, 1321 (1999).
[27] A. Zangwill, *Physics at Surfaces* (Cambridge University Press, Cambridge, England, 1988).
[28] *Electrolyte Data Collection, Viscosity of Nonaqueous Solutions I: Alcohol Solutions*, edited by J. Barthel, R. Neueder, and R. Meier, Chemistry Data Series Vol. XII, (Dechema, Frankfurt, 1997), Pt. 3.
[29] *NBS/NRC Steam Tables: Thermodynamic and Transport Properties and Computer Programs for Vapor and Liquid States of Water in SI Units*, edited by L. Haar, J. S. Gallagher, and G. S. Kell (Hemisphere, Washington DC, 1984).
[30] R. Lovas, G. Macri, and S. Petrucci, J. Am. Chem. Soc. **92**, 6502 (1970).
[31] H. Remy and Z. Elektrochem, Z. Elektrochem. Angew. Phys. Chem. **31**, 88 (1925).
[32] S. E. Ziemniak, M. E. Jones, and K. E. Combs, J. Solution Chem. **601**, 22 (1993).